

# A constraint on light primordial black holes from the interstellar medium temperature

Hyungjin Kim\*

*Department of Particle Physics and Astrophysics,*

*Weizmann Institute of Science, Rehovot 7610001, Israel*

Primordial black holes are a viable dark matter candidate. They decay via Hawking evaporation. Energetic particles from the Hawking radiation interact with interstellar gas, depositing their energy as heat and ionization. For a sufficiently high Hawking temperature, fast electrons produced by black holes deposit a substantial fraction of energy as heat through the Coulomb interaction. Using the dwarf galaxy Leo T, we place an upper bound on the fraction of primordial black hole dark matter. For  $M < 5 \times 10^{-17} M_\odot$ , our bound is competitive with or stronger than other bounds.

## I. INTRODUCTION

Primordial black holes (PBHs) are a viable dark matter candidate. It is minimal in the sense that it does not require new particle state to be added to the spectrum of the standard model. Although it is a compelling candidate, it can only account for all of the dark matter in the mass range of PBHs  $10^{-16} \lesssim M/M_\odot \lesssim 10^{-11}$ . See the recent review [1] for details.

PBHs are decaying dark matter. They evaporate through Hawking radiation [2, 3]. Classical black holes can be described as a thermodynamical system, and the spectrum of emitted particles resembles the blackbody spectrum of temperature  $T = 1/8\pi GM$  with a modification due to gray body factors. Various astrophysical constraints for  $M \lesssim 10^{-16} M_\odot$  exist, based on Hawking evaporation of PBHs. This includes constraints from extragalactic  $\gamma$ -ray flux [4–6], Galactic  $\gamma$ -ray flux [7–12], cosmic microwave background [13–17], cosmic rays [18], and the 21cm absorption [19].

In this paper, we investigate interactions of energetic particles from Hawking radiation in the interstellar medium (ISM). We focus on  $M \lesssim 10^{-16} M_\odot$ . The corresponding Hawking temperature is  $T_{\text{BH}} \gtrsim 50$  keV, and energetic electrons can be easily produced from Hawking evaporation. Once produced, such fast electrons quickly lose most of their energy either through elastic scatterings with charged particles or through ionizing neutral atoms in the gas. A significant fraction of energy

---

\*Electronic address: hyungjin.kim@weizmann.ac.il

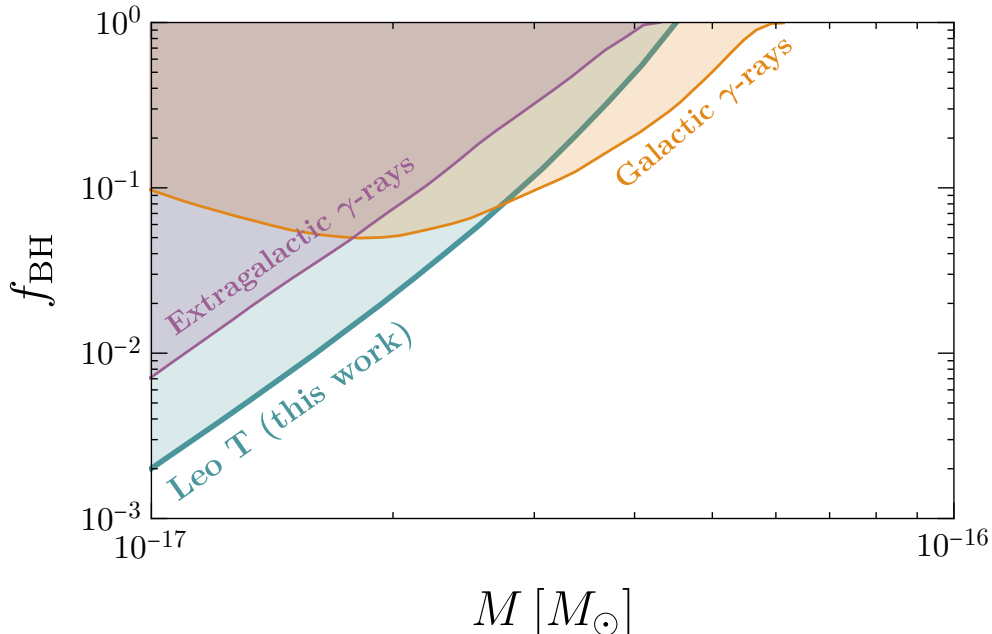


FIG. 1: Constraints on the PBH dark matter fraction  $f_{\text{BH}}$  is shown. Our result is shown as a turquoise shaded region. We also show other constraints from different astrophysical considerations: Galactic  $\gamma$ -ray flux measured by INTEGRAL satellite (orange shaded) [11], and extragalactic  $\gamma$ -ray flux without AGN background (purple shaded) [6] for comparison.

is deposited as heat, and this could contribute to ISM heating as additional source. By considering observed properties of warm neutral medium (WNM) in the dwarf galaxy Leo T, we place a new constraint on the fraction of PBH dark matter for  $M \lesssim 5 \times 10^{-17} M_{\odot}$ . Our main result is shown in Figure 1.

We note that Leo T as well as cold gas clouds in Milky Way have been already investigated to constrain scattering cross sections of WIMP dark matter with the standard model particles [20–23]. In addition, Ref. [24] has recently shown that accreted disk around solar mass PBHs could also heat interstellar gases, and that Leo T can be used to constrain even solar mass PBHs.

The paper is organized in the following order. In Section II, we summarize the observed properties of the dwarf galaxy Leo T. We discuss the cooling and heating of ISM in Section III, and apply them to Leo T to derive a constraint on the PBH dark matter fraction in Section IV. We discuss assumptions made in the analysis in Section V.

## II. LEO T

We only consider the dwarf galaxy Leo T in this paper. It stands out among the other faint dwarf galaxies as it is dark matter dominated, and, at the same time, is gas-rich system. It is located at a distance of 420 kpc, and hosts both cold and warm neutral gases. There is no indication of bulk rotation. The velocity dispersion is  $\sigma = 6.9$  km/sec, which corresponds to  $T_{\text{wnm}} = 6000$  K. The total mass of atomic hydrogen,  $M_{\text{wnm}} = 2.8 \times 10^5 M_{\odot}$ , is extended over  $r_{\text{wnm}} = 350$  pc [25, 26]. From the metallicity measurement of individual stars, iron abundance in Leo T is found as  $[\text{Fe}/\text{H}] = -1.74$  [27].<sup>1</sup>

The profile of atomic hydrogen and free electrons is needed for computation of the gas cooling rate. We assume that the gas is pressure-supported and is confined in the gravitational potential of dark matter halo [28, 29]. The ionization structure is obtained by solving ionization equilibrium,  $\zeta n(H^0) = \alpha_B n(H^+)n(e^-)$ , where  $\zeta$  is photoionization rate due to UV background light, and  $\alpha_B$  is case B recombination rate (excluding a recombination to the ground state). For dark matter, Burkert profile is adopted

$$\rho_{\text{dm}}(r) = \frac{\rho_s}{(1 + r/r_s)(1 + r/r_s)^2}, \quad (1)$$

with best fit parameters for observed Leo T HI column density,  $r_s = 709$  pc and  $\rho_s = 3.8 \text{ GeV}/\text{cm}^3$  [29]. By iteratively solving ionization equilibrium equation while accounting self-shielding of UV background light due to atomic hydrogen, we reproduce the ionization structure of Leo T [23]. Although the profile of atomic hydrogen and free electrons has already obtained in [23], we nevertheless show them in Figure 2 as well as the photoionization rate due to the cosmic UV background for self-contained discussion (cf. Fig. 1 in [23]). We have assumed that cosmic ray ionization has negligible effects on overall ionization structure of Leo T. This will be justified in Section VB

## III. COOLING AND HEATING

The energy transfer rate per unit volume is

$$\frac{dE}{dV dt} = \dot{\mathcal{H}} - \dot{\mathcal{C}}, \quad (2)$$

---

<sup>1</sup>  $[\text{X}/\text{Y}] \equiv \log_{10}(n_X/n_Y) - \log_{10}(n_X/n_Y)_{\odot}$  where  $n_{X,Y}$  is the number density of species X and Y, and the subscript  $\odot$  represents the solar abundance.

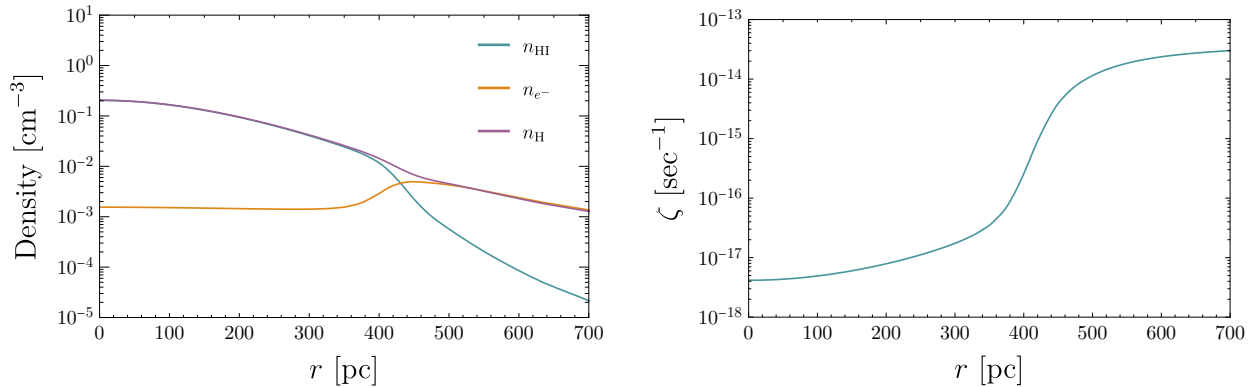


FIG. 2: (Left) Profiles of atomic hydrogen and free electrons in Leo T, obtained from the procedure described in the main text. We choose  $T_{\text{wnm}} = 6000$  K,  $M_{\text{wnm}} = 2.8 \times 10^5 M_{\odot}$ ,  $r_{\text{wnm}} = 350$  pc,  $v_s = 30$  km/sec, and  $r_s = 709$  pc [25, 29]. This result was also obtained in [23], but shown here for the self-contained discussion. (Right) The total photoionization rate in Leo T due to cosmic UV background [28, 30].

where  $\dot{\mathcal{H}}$  is the total heating rate, and  $\dot{\mathcal{C}}$  is the total cooling rate. We derive a new bound on the fraction of PBH dark matter by imposing

$$\frac{1}{V} \int dV \dot{\mathcal{H}}_{\text{BH}} < \frac{1}{V} \int dV \dot{\mathcal{C}}, \quad (3)$$

where  $\dot{\mathcal{H}}_{\text{BH}}$  is the heating rate due to PBH Hawking radiation. The volume integration is performed over the volume of system under the consideration; in our case, this would be the volume of WNM in Leo T. Although there are other heating sources such as cosmic ray and photoionization heating, we ignore them for a conservative estimate. We derive  $\dot{\mathcal{C}}$  in the next section,  $\dot{\mathcal{H}}_{\text{BH}}$  in Section III B, and present the result in Section IV.

### A. Cooling

Cooling is a process that extracts energy from the system. For the interstellar medium, it is dominated by photon emission. A variety of processes contribute to the gas cooling. It includes rotational and vibrational excitations of molecules, fine structure transitions of metals, Lyman- $\alpha$  transition, and bremsstrahlung of ions. For warm neutral medium of  $n_{\text{H}} \sim 0.1 \text{ cm}^{-3}$ ,  $T_{\text{wnm}} \simeq 6000$  K and  $x_e = n_e/n_{\text{H}} \sim \mathcal{O}(10^{-2})$ , most important coolants are metal line transitions, and perhaps, Ly $\alpha$  transition and ro-vibrational excitation of  $\text{H}_2$  in a metal poor system. Among metals,  $\text{C}^+$ ,  $\text{O}^0$ , and  $\text{Si}^+$  lines are dominant coolants at the temperature and electron density of our primary interest.

Since the cooling takes place through atomic and molecular de-excitation, it can be written as

$$\dot{C} = \sum_{u>\ell} n_u A_{u\ell} \omega_{u\ell}, \quad (4)$$

where  $n_u$  is the density of excited state  $u$ ,  $\omega_{u\ell} = \omega_u - \omega_\ell$  is the level spacing, and  $A_{u\ell}$  is the spontaneous decay rate. We use the subscript  $u$  and  $\ell$  to indicate upper and lower atomic levels, respectively. We ignore the stimulated emission since the photon occupation number at any relevant frequencies is smaller than unity. This expression assumes that all emitted photons from atomic and molecular de-excitation can escape the system, which is a valid assumption for photons from fine structure transitions in WNM. To compute the cooling rate, we will use an approximate expression given in Eq. (8) instead of Eq. (4). A derivation is detailed in the next paragraph with two-level system and uninterested readers can directly jump to Eq. (8).

The excited state density  $n_u$  is needed to compute  $\dot{C}$ . Most cooling arises from transitions among a few low-lying states. Consider two-level system for simplicity. The cooling transition in  $C^+$ , one of the major coolants, can be accurately described by two-level system. The population of excited state is obtained from the collisional equilibrium condition,

$$\frac{dn_1}{dt} = n_0 C_{01} - n_1 (C_{10} + A_{10}) = 0. \quad (5)$$

The collisional de-excitation rate  $C_{10}$  is

$$C_{10} = \sum_c n(c) k_{10}(c), \quad (6)$$

where  $n(c)$  is the density of collision partner  $c$  ( $c = e^-, H^0, p^+, He^0, \dots$ ), and  $k_{10}(c) = \langle \sigma v \rangle_{1 \rightarrow 0}(c)$  is a thermal-averaged de-excitation rate. The subscript 0 and 1 denote the ground and excited state, respectively. The collisional excitation and de-excitation rate are related by the detailed balance,  $C_{01} = C_{10}(g_1/g_0)e^{-\omega_{10}/T}$ . The excited population is  $n_1/n_0 = C_{01}/(C_{10} + A_{10})$ , and therefore, the cooling rate in the two-level system is

$$\dot{C} = n_0 C_{01} \omega_{10} \left[ 1 + \sum_c \frac{n(c)}{n_{\text{crit}}(c)} \right]^{-1}, \quad (7)$$

where we define the critical density as  $n_{\text{crit}}(c) = A_{10}/k_{10}(c)$ ; this is the density at which the collisional de-excitation rate and spontaneous decay rate becomes equal. In the limit  $n(c) \ll n_{\text{crit}}(c)$ , the cooling rate is the same as the collisional excitation rate weighted by the energy level difference.

For  $N$ -level system, it is a straightforward to show

$$\dot{C} \approx \sum_u n_0 C_{0u} \omega_{u0}, \quad (8)$$

when  $n(c) \ll n_{\text{crit}}(c)$ . In what follows, we always assume  $n(c) \ll n_{\text{crit}}(c)$  and use Eq. (8) to compute the cooling rate.

To grasp an idea of how large the cooling rate is, let us take an example of  $\text{C}^+$ . The strongest cooling line is the  $158\mu\text{m}$  transition between two lowest-lying states,  $^2P_{3/2} \rightarrow ^2P_{1/2}$ . The energy of photon is  $\omega_{10} = 2\pi/(158\mu\text{m}) = 8 \times 10^{-3} \text{ eV}$ , and the spontaneous decay rate is  $A_{10} = 2 \times 10^{-6} \text{ sec}^{-1}$ . The rate coefficients at  $T = 6000 \text{ K}$  are

$$k_{10}(e^-) = 5 \times 10^{-8} \text{ cm}^3/\text{sec}, \quad (9)$$

$$k_{10}(H^0) = 2 \times 10^{-9} \text{ cm}^3/\text{sec}, \quad (10)$$

which are obtained from the fitting formula in [31]. The critical density is  $n_{\text{crit}}(e^-) = 50 \text{ cm}^{-3}$  and  $n_{\text{crit}}(H^0) = 10^3 \text{ cm}^{-3}$ , confirming  $n(c) \ll n_{\text{crit}}(c)$ . The cooling rate is therefore

$$\dot{C}_{\text{CII}} \simeq n_0 C_{01} \omega_{10} \sim 6 \times 10^{-27} \text{ erg/cm}^3/\text{sec} \times \left( \frac{\mathcal{A}_C}{10^{-4}} \right) \left( \frac{n_H}{1 \text{ cm}^{-3}} \right)^2, \quad (11)$$

where we have chosen  $x_e = x_p = 10^{-2}$ , and  $\mathcal{A}_C = n_0/n_H$  is the carbon abundance normalized with the total hydrogen density. The carbon abundance in the solar neighborhood is  $\mathcal{A}_C \simeq 10^{-4}$ . The cooling rate from the other metal lines can be computed in the same way, and all of them is proportional to the gas-phase metal abundance  $\mathcal{A}_X$ . Due to dust grains in interstellar medium, however, gas-phase metals can condense to a solid form, and therefore, the gas-phase abundance is depleted from the stellar metal abundance. This is called interstellar depletion. A complication related to the gas-phase metallicity will be discussed in Section V. We refer readers to [31–33] for general discussions on the cooling and heating of interstellar medium.

We comment on two other cooling sources, which do not directly depend on the metal abundance. This includes ro-vibrational transitions in molecular hydrogen  $\text{H}_2$ , and the Lyman- $\alpha$  transition. The cooling rate due to  $\text{H}_2$  can be parametrized as

$$\dot{C}_{\text{H}_2} = \sum_c n(c)n(\text{H}_2)\Lambda_{\text{H}_2}(c). \quad (12)$$

Analytic fits for  $\Lambda_{\text{H}_2}$  are given in [34, 35] for  $c = e, \text{H}^0, \text{H}^+, \text{He}$ . The abundance of molecular hydrogen can be obtained by solving chemical network. Instead, we use an analytic expression for  $\text{H}_2$  abundance obtained from the reduced chemical network [36]. On the other hand, the Ly $\alpha$  cooling rate is [32, 37, 38]

$$\dot{C}_{\text{Ly}\alpha} = n_{\text{HI}}n_e \left[ 7.5 \times 10^{-19} e^{-118348 \text{ K}/T} / (1 + T_5^{1/2}) \right] \text{ erg cm}^{-3} \text{ s}^{-1}, \quad (13)$$

where  $T_5 \equiv T/10^5 \text{ K}$ . The exponent arises from the energy level difference  $\omega_{10} \simeq 10.2 \text{ eV}$ . Although the excitation rate is exponentially suppressed, Ly $\alpha$  cooling dominates the metal cooling for  $T > 10^4$

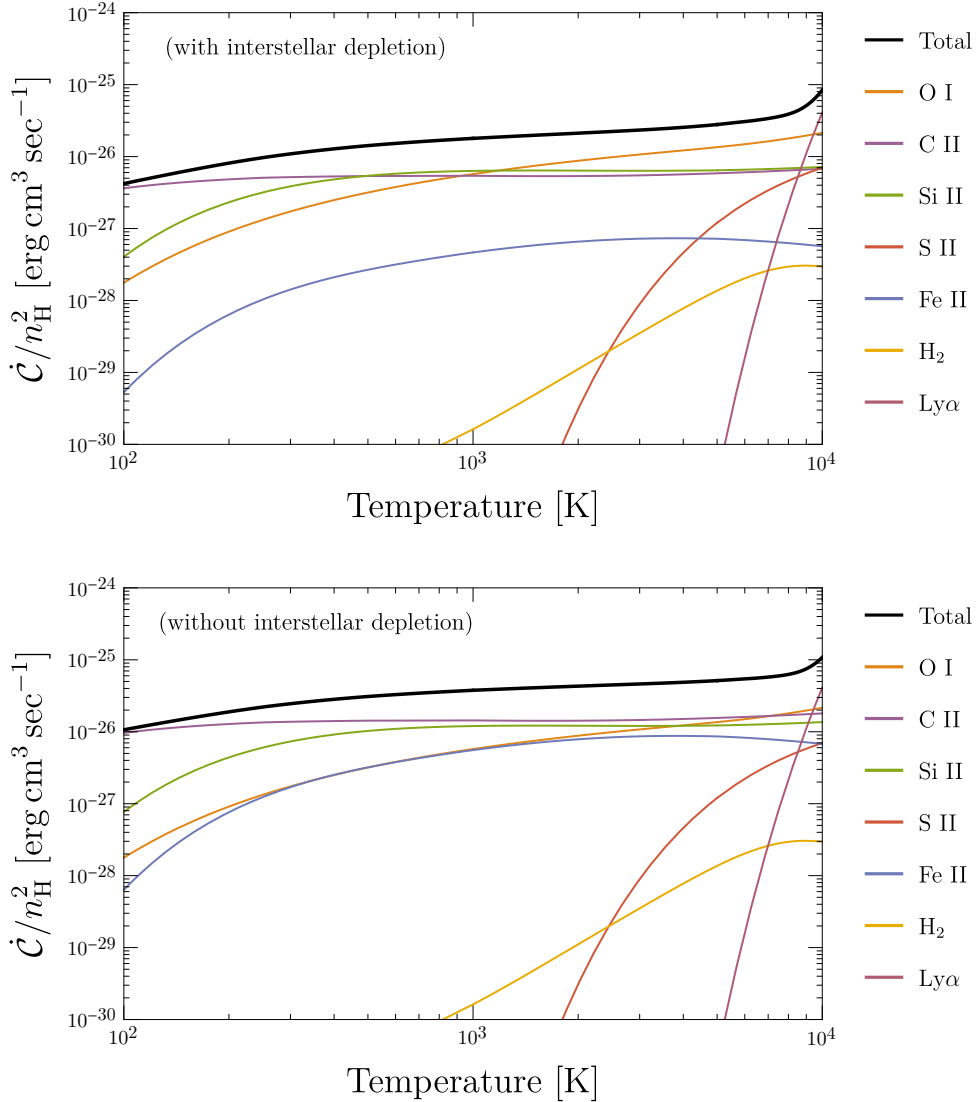


FIG. 3: (Top) The cooling function at the solar metallicity  $Z = Z_{\odot}$  with depleted elemental abundance. We choose  $x_e = x_p = 10^{-2}$ ,  $x_{\text{H}_2} = n(\text{H}_2)/n_{\text{H}} = 10^{-6}$ ,  $n_{\text{H}} = 1 \text{ cm}^{-3}$ . (Bottom) The cooling function at the solar metallicity, while the metal abundance is chosen before the interstellar depletion. All the other parameters are chosen the same. Since the depletion of iron in the local interstellar medium is significant ( $>90\%$ ), it could be as important as the other elements in any environment where the depletion can be neglected. See the main text for details.

K since the hydrogen is more abundant than metals, and the Lyman- $\alpha$  photon is much more energetic compared to the photon coming from fine structure transitions. The Ly $\alpha$  and H $_2$  cooling could be sub-leading or even comparable to the metal cooling in a metal poor environment under a certain condition. In Leo T, we find that Ly $\alpha$  and H $_2$  cooling remain as sub-leading contributions to the total cooling rate. We will discuss this in Section V C.

In Figure 3, we show the total cooling rate as well as individual contributions. We show the cooling curves for the solar metal abundance [39] with and without interstellar depletion [31, 40]. For both figures, we choose  $x_e = x_p = 10^{-2}$ ,  $x(\text{H}_2) = n(\text{H}_2)/n_{\text{H}} = 10^{-6}$ , and  $n_{\text{H}} = 1 \text{ cm}^{-3}$ . The electron-impact excitation rate coefficients  $k_{u\ell}(e^-) = \langle \sigma v \rangle_{u \rightarrow \ell}(e^-)$  are taken from Stout atomic library [41].<sup>2</sup> Since we are interested in cooling of WNM, hydrogen-impact excitation could be equally important. We have used Barinovs et al. [48] for  $\text{C}^+$  and  $\text{Si}^+$  and Lique et al. for  $\text{O}^0$  [49] for the hydrogen-impact excitation rates  $k_{u\ell}(\text{H}^0) = \langle \sigma v \rangle_{u \rightarrow \ell}(\text{H}^0)$ . Since the quantum mechanical computation of hydrogen-impact excitation of  $\text{C}^+$  and  $\text{Si}^+$  is only available for limited temperature range,  $15 \text{ K} \leq T \leq 2000 \text{ K}$ , we extrapolate the rate coefficients to  $T_{\text{wnm}} = 6000 \text{ K}$  based on the fitting formulae given in [48]. We use analytic fits given in Appendix A for  $\text{H}^0\text{-O}^0$  collision. Most dramatic change in the cooling rate with and without interstellar depletion arises from Fe II lines since the abundance of iron is depleted more than 90 % in the local interstellar medium relative to the solar abundance [31, 40]. The difference in the total cooling rate with and without depletion remains less than a factor three for the shown temperature range.

## B. Heating

We consider the heating from Hawking radiations. Primordial black holes could inject energetic particles to the interstellar medium. The particle production rate per internal degree of freedom per unit volume is

$$dn = n_{\text{dm}} \frac{(\sigma_{\text{abs}} v)}{e^{\omega/T} \pm 1} \frac{d^3 k}{(2\pi)^3} = n_{\text{dm}} \frac{\Gamma_{\text{abs}}}{2\pi} \frac{d\omega}{e^{\omega/T} \pm 1}, \quad (14)$$

where  $\sigma_{\text{abs}}$  is an absorption cross section due to the black hole,  $\Gamma_{\text{abs}} = \sigma_{\text{abs}} k^2 / \pi$  is the absorption probability of emitted particles, and  $n_{\text{dm}} = f_{\text{BH}}(\rho_{\text{dm}}/M)$  is the number density of PBHs with the PBH dark matter fraction  $f_{\text{BH}}$ . We assume that PBHs are Schwarzschild black holes with a  $\delta$ -function mass distribution. The absorption probability can be obtained by numerically solving wave equation under black hole geometries [50–52]. Instead, we use the publicly available code `blackHawk` [53] to compute the spectrum.

Once electrons are produced, their energy is lost by elastic scatterings with other charged particles and by ionization/excitation of neutral atoms. An energy loss due to elastic scatterings increases thermal energy of the medium, and hence, contributes to the heating rate. In addition,

<sup>2</sup> The electron-impact excitation rate for each element is originally obtained in the following references:  $\text{C}^+$  [42],  $\text{O}^0$  [43, 44],  $\text{Si}^+$  [45],  $\text{Fe}^+$  [46],  $\text{S}^+$  [47].



secondary electrons produced from the ionization of primary electron also contribute to the heating rate. Let us define  $f_{\text{heat}}(\omega)$  as a fraction of primary electron's energy that is deposited as heat. Then the heating rate due to electrons and positrons is

$$\dot{\mathcal{H}}_{\text{BH}} = \int d\omega (\omega - m_e) f_{\text{heat}}(\omega) \frac{d\dot{n}_{e^\pm}}{d\omega}. \quad (15)$$

The heating rate from Hawking radiation is equal to the convolution of the total kinetic energy carried by emitted electrons and positrons with the heat deposition efficiency. For the heat deposition efficiency  $f_{\text{heat}}(\omega)$ , we adopt the analytic fit given in the Appendix of [54], which is based on the numerical simulation [55]. This fitting formula agrees with numerical results from a more recent Monte Carlo simulation [56]. Above 1 keV, the heat deposition efficiency becomes almost constant, and the energy of primary electron is more or less equally distributed as heat, ionization, and excitation [56].

#### IV. RESULT

We apply our discussion to the dwarf galaxy Leo T. For the metal abundance, we take the solar abundance without the interstellar depletion, and rescale them according to the observed metallicity,

$$\mathcal{A}_X = 10^{[\text{X}/\text{H}]} \mathcal{A}_{X,\odot} \approx 10^{[\text{Fe}/\text{H}]} \mathcal{A}_{X,\odot}, \quad (16)$$

where  $\mathcal{A}_{X,\odot}$  is the solar abundance of metal species  $X$  without depletion. We assume  $[\text{X}/\text{H}] = [\text{Fe}/\text{H}]$  for all metal elements  $X$  under the consideration, i.e. the elemental abundance of the gas in Leo T follows solar abundance pattern. We use  $[\text{Fe}/\text{H}] = -1.74$  [27]. Using the profile of atomic hydrogen and electron as an input, we compute the volume-averaged cooling rate as

$$\dot{\mathcal{C}} \simeq 7 \times 10^{-30} \text{ erg/cm}^3/\text{sec}. \quad (17)$$

For the PBH mass smaller than a few times  $10^{-17} M_\odot$ , we find the average heating rate as

$$\dot{\mathcal{H}}_{\text{BH}} \simeq (3 \times 10^{-27} \text{ erg/cm}^3/\text{sec}) \times (10^{-17} M_\odot/M)^3. \quad (18)$$

By comparing the volume-averaged cooling and heating rate Eq. (15), we place an upper bound on the PBH dark matter fraction as shown in Figure 1. Our result based on the heating of ISM from fast electrons are shown as turquoise shaded region. We also show other constraints, arising from extragalactic  $\gamma$ -ray flux [6] (purple shaded) and Galactic  $\gamma$ -ray flux [11] (orange shaded)

for comparison. The constraint is shown for  $M \geq 10^{-17} M_\odot$ . Below this mass, we expect that the constraint on the PBH dark matter fraction scales as  $f_{\text{BH}} \propto M^3$  for the following reason. For this mass range, Hawking temperature becomes larger than the rest mass of electron, and the heating rate in this case can be approximated as  $\dot{\mathcal{H}}_{\text{BH}} \approx n_{\text{dm}} \bar{f}_{\text{heat}} P_{e^\pm}$  where  $\bar{f}_{\text{heat}}$  is the asymptotic value of heat deposition fraction at high energy  $\sim \mathcal{O}(0.1)$ , and  $P_{e^\pm}$  is the total power radiated through electrons and positrons from a black hole. The total power can be approximated as  $P_{e^\pm} \sim A_{\text{BH}} T_{\text{BH}}^4 \propto T_{\text{BH}}^2$  with a surface area of black hole  $A_{\text{BH}} = 4\pi r_s^2$ , while  $n_{\text{dm}} = \rho_{\text{dm}}/M$ . Therefore,  $\dot{\mathcal{H}}_{\text{BH}} \propto T_{\text{BH}}^2/M \propto 1/M^3$ , and thus, we expect the bound should scale as  $f_{\text{BH}} \propto M^3$  for smaller mass as long as thermalization time scale is shorter than the cooling time scale, which will be discussed in Section V E.

## V. DISCUSSION

In this section, we discuss details related to the computation of cooling and heating rate, intended to justify some simplifications and assumptions made.

### A. Metallicity

The cooling is dominated by metal lines. The cooling rate from each metal element is proportional to the gas-phase abundance  $\mathcal{A}_X$ . For this, we have used Eq. (16),  $\mathcal{A}_X/\mathcal{A}_{X,\odot} \approx 10^{[\text{Fe}/\text{H}]}$ . Two assumptions are made: (i) there is negligible interstellar depletion such that the gas-phase metallicity is similar to the stellar metallicity and (ii) the chemical composition pattern in Leo T follows solar composition pattern, i.e.  $[\text{X}/\text{H}] \simeq \text{constant}$  for all elements under consideration.

Since the depletion of gas-phase elements takes place as a dust grain captures gas-phase element, we naturally expect that the degree of depletion is proportional to the dust abundance. For a system following the solar abundance pattern, the gas-phase abundance can be approximated as [36]

$$\mathcal{A}_X \approx \mathcal{A}_{X,\odot} (Z/Z_\odot) [1 - \delta_X Z_d (Z_\odot/Z)], \quad (19)$$

where  $Z_d$  is the dust-to-gas mass ratio normalized as  $Z_d = 1$  in the local ISM, and  $\delta_X$  is a degree of depletion at the solar metallicity.

The dust-to-gas ratio scales linearly with metallicity,  $Z_d \propto Z$ , for systems with near-solar metallicity [57]. For metal-poor galaxies, recent studies [58, 59] have shown that the trend of dust-to-gas ratio versus metallicity deviates from this simple linear relation, and in fact, Ref. [58] has found a steeper dependence on metallicity,  $Z_d \propto Z^{3.1}$ . The transition takes place at  $Z/Z_\odot \simeq 0.2$  [58].

For the system with  $Z/Z_{\odot} \simeq 0.01$ , which is commonly observed in ultrafaint dwarf galaxies, we find  $Z_d(Z_{\odot}/Z) \sim 10^{-3}$ . In the local ISM, iron is most significantly depleted, and even in this case,  $\delta_{\text{Fe}} \sim 0.9$  [40]. Therefore, we can safely ignore interstellar depletion in low-metallicity systems like Leo T.

Another assumption made in Eq. (16) is that the elemental composition in Leo T is the same as solar composition pattern. In the other words, we have assumed that  $[X/H] = \log_{10}(n_X/n_H)_{\text{LeoT}} - \log_{10}(n_X/n_H)_{\odot} = \text{constant}$  for all  $X$ , indicating that the metal abundance of any given metal species in Leo T is suppressed by the common factor relative to the solar abundance of  $X$ . This assumption is not necessarily true for certain systems. The observations of ultrafaint dwarf galaxies have revealed that the alpha-elements, such as O and Si, are enhanced relative to the solar abundance pattern, i.e.  $[\alpha/\text{Fe}] > 0$ .

This enhancement in  $\alpha$ -elements is the result of the chemical enrichment due to Type II supernovae (SNe) explosions. It is well known that Type II SNe explosions produce a large amount of  $\alpha$ -elements, resulting in  $[\alpha/\text{Fe}] > 0$ , while Type Ia SNe explosions mainly produce iron-peak elements, and thus, raising  $[\text{Fe}/\text{H}]$  and lowering  $[\alpha/\text{Fe}]$ . At the same time, a minimum time of  $\sim 100$  Myr is required [60, 61] for Type Ia SNe to explode, and therefore, we may understand the enhancement in  $\alpha$ -elements as an indication of star formation lasted less than 100 Myr. From the study of seven ultrafaint dwarf galaxies, Ref. [62] found a sharp drop of  $[\alpha/\text{Fe}]$  around  $[\text{Fe}/\text{H}] \sim -2.3$ . See also [63] for a model of chemical evolution of ultrafaint dwarf galaxies and [64] for numerical simulation. Since Leo T has a relatively large metallicity  $[\text{Fe}/\text{H}] = -1.74$  [27] and also hosts a recent star formation [65–67], it is reasonable to expect the elemental abundance of Leo T closely follows solar abundance pattern,  $[\alpha/\text{Fe}] \simeq 0$ . See the recent review [68] for further discussions.

Finally, we comment on a numerical difference in the cooling rate compared to the previous works [23, 24]. We have found a factor three larger cooling rate compared to what was found in [23]. This numerical difference can be attributed to the metallicity used in the computation of the cooling rate as well as the effect of interstellar depletion. For the metallicity used in [23] ( $[\text{Fe}/\text{H}] = -1.99$  [69]) and for the depleted elemental abundance, we obtain the averaged cooling rate reasonably close to the one presented in [23] ( $\dot{C} \sim 2 \times 10^{-30} \text{ erg/cm}^3/\text{sec}$ ).

## B. Cosmic ray ionization

When determining the ionization structure of Leo T, we have only accounted ionization due to cosmic UV background, while ignoring a potential contribution from cosmic rays. In order to justify

this, we have to make sure that the cosmic ray ionization rate is smaller than  $\sim 4 \times 10^{-18} \text{ sec}^{-1}$ .

The cosmic ray ionization produces secondary electrons with energies  $\sim 30 \text{ eV}$  [37]. Similar to fast electrons from Hawking radiation, this secondary electron could also contribute to the heating of ISM. The heating rate is [37]

$$\begin{aligned} \dot{\mathcal{H}}_{\text{cr}} &= [n(\text{H}^0) + n(\text{He}^0)] \zeta_{\text{cr}} E_h \simeq 10^{-27} \text{ erg/s} \times \zeta_{-16} [n(\text{H}^0) + n(\text{He}^0)] \left[ 1 + 4 \left( \frac{x_e}{x_e + 0.07} \right)^{1/2} \right] \\ &\rightarrow (2 \times 10^{-28} \text{ erg/cm}^3/\text{sec}) \times \zeta_{-16}, \end{aligned} \quad (20)$$

where  $E_h$  is the average heat per ionization, and  $\zeta_{-16} \equiv \zeta_{\text{cr}}/10^{-16} \text{ sec}^{-1}$ . The second line is obtained after averaging over the volume of WNM. By comparing averaged cooling rate Eq. (17), we find  $\zeta_{\text{cr}} < 3 \times 10^{-18} \text{ sec}^{-1}$ . Therefore, we indirectly conclude that the cosmic ray ionization rate consistent to the observed temperature of WNM in Leo T has negligible effects on ionization fraction  $x_e$ .

### C. Interstellar radiation field

As we have briefly mentioned in Section III A, the cooling due to molecular hydrogen may be comparable to the metal cooling in low metallicity environment because it does not directly depend on the metallicity. This can be seen from the cooling curves in Figure 3. On the other hand, the abundance of  $\text{H}_2$  is determined by a network of chemical reactions. Two important chemical reactions that suppress the abundance of  $\text{H}_2$  are the photodissociation of molecular hydrogen,  $\text{H}_2 + \gamma \rightarrow \text{H} + \text{H}$ , and the photodetachment of hydrogen ion,  $\text{H}^- + \gamma \rightarrow \text{H} + e$ , all due to UV interstellar radiation field (ISRF). Therefore, the strength of ISRF is crucial to determine  $n(\text{H}_2)$ , and thus, the cooling due to molecular hydrogen.

To infer the strength of ISRF, we make use of equipartition of energy. In the local ISM, the energy density stored in thermal gas and in starlight are surprisingly similar;  $\rho_{\text{thermal}} \sim \rho_{\text{starlight}} (\omega < 13.6 \text{ eV}) \sim 0.5 \text{ eV/cm}^3$  [31, 70]. On the other hand, the average thermal energy of WNM in Leo T is  $\rho_{\text{thermal}} = \frac{3}{2} \langle n_{\text{HI}} \rangle T_{\text{wnm}} \simeq 0.05 \text{ eV/cm}^3$ , ten times smaller than the kinetic energy density in the local ISM. We assume that the strength of ISRF is suppressed by the same amount, while the spectral shape remains the same. In such case, the cooling due to molecular hydrogen remains sub-dominant. For stronger ISRF, the  $\text{H}_2$  cooling becomes negligible since  $\text{H}_2$  abundance is more strongly suppressed, while for an order of magnitude weaker ISRF strength relative to the value inferred from equipartition, the total averaged cooling rate increases by  $\sim 50\%$ , signaling that the  $\text{H}_2$  cooling becomes comparable to the metal cooling rate. Therefore, our result remains intact for

a wide range of ISRF strength unless it is smaller by more an order of magnitude than what is inferred from equipartition theorem. We also note that the spectrum of ISRF in metal poor galaxies is harder compared to Galactic ISRF [71], which may further suppress H<sub>2</sub> abundance.

#### D. Photoelectric heating

Can photons from Hawking evaporation provide additional heating? Photons could also heat ISM by producing photoelectrons. The heating rate can be computed as

$$\dot{\mathcal{H}} \sim n_{\text{HI}} \int d\omega (\omega - I_{\text{H}}) \sigma_{\text{H}}(\omega) f_{\text{heat}}(\omega) \frac{dn_{\gamma}}{d\omega}, \quad (21)$$

where  $I_{\text{H}} = 13.6 \text{ eV}$  is the ionization potential of hydrogen,  $\sigma_{\text{H}}$  is photoionization cross section, and  $dn_{\gamma}/d\omega$  is the photon number density in  $[\omega, \omega + d\omega]$  frequency interval. The photoelectric cross section above keV scales as  $\sigma_{\text{H}} \propto \omega^{-3.5}$ , while  $dn_{\gamma}/d\omega$  at  $\omega < T_{\text{BH}}$  scales as  $dn_{\gamma}/d\omega \propto \omega^4$  due to the gray body factor for spin one bosons [50]. This allows us to estimate the heating rate by evaluating the integrand at the peak of  $dn_{\gamma}/d\omega$ , which is  $\omega \sim 2\pi T_{\text{BH}}$ . Using  $\sigma_{\text{H}} \simeq 5 \times 10^{-17} \text{ cm}^2 (I_{\text{H}}/\omega)^{3.5}$ , and  $dn_{\gamma}/d\omega = N_{\text{dm}}(dN_{\gamma}/d\omega dt)$  with dark matter column density  $N_{\text{dm}} \sim n_{\text{dm}} r_s$  and  $(dN_{\gamma}/d\omega dt)_{\text{peak}} \simeq 10^{21} \text{ GeV}^{-1} \text{ sec}^{-1}$  [52], we find  $\dot{\mathcal{H}} \sim (10^{-40} \text{ erg/cm}^3/\text{sec}) \times (n_{\text{HI}}/1 \text{ cm}^{-3})(M/10^{-16} M_{\odot})^{1/2}$ . Therefore, photons from Hawking evaporation have negligible heating effects.

#### E. Time scales

Our result is based on the heating rate Eq. (15). This expression assumes that the energy of primary electron is instantaneously injected into the ISM as a thermal energy. This assumption is justified only if the thermalization time scale is shorter than the cooling time scale. The cooling time scale is

$$t_{\text{cool}} = \frac{E_{\text{th}} n}{\dot{\mathcal{C}}} \simeq 0.4 \text{ Gyr}, \quad (22)$$

where we have used the average gas density  $n = 0.07 \text{ cm}^{-3}$  in WNM, the average cooling rate Eq. (17), and the thermal energy  $E_{\text{th}} = (3/2)T_{\text{wnm}}$ . On the other hand, the thermalization time scale can be obtained from the following electron energy evolution equation,

$$\frac{dE}{dt} \simeq - \left( \frac{\partial E}{\partial t} \right)_{\text{el}} - \left( \frac{\partial E}{\partial t} \right)_{\text{ion}} + \dots, \quad (23)$$

where  $(\partial E/\partial t)_{\text{el}}$  and  $(\partial E/\partial t)_{\text{ion}}$  are the energy loss due to elastic scattering and ionization, respectively. Thermalization time scale through the elastic scattering can be defined as

$$t_{\text{th}} = \frac{E}{(\partial E/\partial t)_{\text{el}}} \simeq \frac{2}{n_e \sigma_{\text{tr}} v_{\text{rel}}} \sim (0.03 \text{ Gyr}) \times \left( \frac{E}{\text{MeV}} \right) \left( \frac{1.5 \times 10^{-3} \text{ cm}^{-3}}{n_e} \right), \quad (24)$$

where  $\sigma_{\text{tr}} \equiv \int d\Omega (1 - \cos \theta) d\sigma/d\Omega \simeq 8\pi\alpha^2 \ln \Lambda / (m_e E)$  is the transport (momentum transfer) cross section in the relativistic regime,  $E$  is the kinetic energy, and  $\ln \Lambda \simeq \ln(2p_{\text{CM}}v/\omega_p)$  is the Coulomb logarithm with the plasma frequency  $\omega_p = (4\pi\alpha n_e/m_e)^{1/2}$  [72]. The above expression is valid for the relativistic regime. In the nonrelativistic regime, the thermalization time scale scales as  $t_{\text{th}} \propto E^{3/2}$ . Note that the average kinetic energy of electrons from PBH is  $\langle E \rangle \sim 3T_{\text{BH}} \simeq 2 \text{ MeV} (10^{-17} M_{\odot}/M)$ . Therefore, elastic scattering is sufficiently strong such that it thermalizes MeV scale energy within the cooling time scale.

Not only the elastic scattering, but also ionization contributes to thermalization in a significant way [55]. Each ionization process divides the energy of primary electron into smaller secondary electron energies. The mean energy of secondary electron is  $\sim \mathcal{O}(10)$  eV for MeV scale primary electron [73], and thus, the secondary electron can be instantaneously thermalized on time scale of interest. The time scale of ionization energy loss is

$$t_{\text{ion}} = \frac{E}{(\partial E/\partial t)_{\text{ion}}} \sim (3 \times 10^{-3} \text{ Gyr}) \times \left( \frac{0.06 \text{ cm}^{-3}}{n_{\text{HI}}} \right) \left( \frac{E}{\text{MeV}} \right), \quad (25)$$

where  $(\partial E/\partial t)_{\text{ion}} \simeq n_{\text{HI}} (2\pi\alpha^2/m_e) \log(m_e^2 \gamma^3 / 2I_H^2)$  is the ionization energy loss rate in the relativistic regime [74]. As long as  $M \gtrsim 10^{-19} M_{\odot}$ , the above time scale is much shorter than the cooling time scale, and thus, we can assume that a significant fraction of energy is thermalized before the cooling is initiated.

## VI. SUMMARY

We have considered the interstellar medium as a probe of primordial black hole dark matter. We have computed the total cooling rate in Leo T, considering various processes such as metal line transitions, transitions in molecular hydrogen levels, and the Ly $\alpha$  transition. By comparing the cooling rate with the heating rate due to electrons emitted from PBHs, we have obtained an upper limit on the PBH dark matter fraction  $f_{\text{BH}}$ , that is competitive with or stronger than other existing constraints for  $M \lesssim 5 \times 10^{-17} M_{\odot}$  (See Figure 1).

### Acknowledgments

We would like to thank Kfir Blum, Joshua Eby, Fatemeh Elahi, and Sarah Schon for useful discussions. The author especially thanks Kfir Blum and Joshua Eby for helpful suggestions and comments on the first version of the manuscript, Steven R. Furlanetto for providing his numerical results on the energy deposition fraction of fast electrons, and François Lique for the clarification on the hydrogen-impact collision data of atomic oxygen. The author thanks the GGI Institute for Theoretical Physics and CERN for hospitality during “Next Frontiers in the Search for Dark Matter” and “Axions in the Lab and in the Cosmos” workshops, during which this work was conceived.

### Appendix A: Analytic fits for the hydrogen-impact excitation of atomic oxygen

For the hydrogen-impact collision of atomic oxygen, we have used LAMDA database [75].<sup>3</sup> The collision data has been obtained in Lique et al. [49]. The data is obtained for 10 K – 8000 K and can be fitted with

$$k_{21}(H^0) = 1.087 \times 10^{-10} \left[ 1 + 2.016 \times T_3^{1.097-0.129 \ln T_3} \right] \text{cm}^3/\text{sec}, \quad (\text{A1})$$

$$k_{20}(H^0) = 4.933 \times 10^{-11} \left[ 1 + 7.368 \times T_3^{0.599-0.064 \ln T_3} \right] \text{cm}^3/\text{sec}, \quad (\text{A2})$$

$$k_{10}(H^0) = 1.068 \times 10^{-8} \left[ 1 - 0.950 \times T_3^{-0.023-0.003 \ln T_3} \right] \text{cm}^3/\text{sec}. \quad (\text{A3})$$

For  $1000 \text{ K} < T < 8000 \text{ K}$ , the error remains less than three percent. We use the above fitting formula to compute the cooling rate due to hydrogen-impact excitation of atomic oxygen.

- 
- [1] B. Carr, K. Kohri, Y. Sendouda, and J. Yokoyama, (2020), arXiv:2002.12778.
  - [2] S. Hawking, *Nature* **248**, 30 (1974).
  - [3] S. Hawking, *Commun. Math. Phys.* **43**, 199 (1975), [Erratum: *Commun.Math.Phys.* 46, 206 (1976)].
  - [4] B. Carr, K. Kohri, Y. Sendouda, and J. Yokoyama, *Phys. Rev. D* **81**, 104019 (2010), arXiv:0912.5297.
  - [5] A. Arbey, J. Auffinger, and J. Silk, *Phys. Rev. D* **101**, 023010 (2020), arXiv:1906.04750.
  - [6] G. Ballesteros, J. Coronado-Blázquez, and D. Gaggero, (2019), arXiv:1906.10113.
  - [7] B. Carr, K. Kohri, Y. Sendouda, and J. Yokoyama, *Phys. Rev. D* **94**, 044029 (2016), arXiv:1604.05349.
  - [8] W. DeRocco and P. W. Graham, *Phys. Rev. Lett.* **123**, 251102 (2019), arXiv:1906.07740.

---

<sup>3</sup> See <https://home.strw.leidenuniv.nl/~moldata/>.

- [9] R. Laha, Phys. Rev. Lett. **123**, 251101 (2019), arXiv:1906.09994.
- [10] B. Dasgupta, R. Laha, and A. Ray, (2019), arXiv:1912.01014.
- [11] R. Laha, J. B. Muñoz, and T. R. Slatyer, Phys. Rev. D **101**, 123514 (2020), arXiv:2004.00627.
- [12] M. H. Chan and C. M. Lee, (2020), arXiv:2007.05677.
- [13] S. Clark, B. Dutta, Y. Gao, L. E. Strigari, and S. Watson, Phys. Rev. D **95**, 083006 (2017), arXiv:1612.07738.
- [14] P. Stöcker, M. Krämer, J. Lesgourgues, and V. Poulin, JCAP **03**, 018 (2018), arXiv:1801.01871.
- [15] H. Poulter, Y. Ali-Haïmoud, J. Hamann, M. White, and A. G. Williams, (2019), arXiv:1907.06485.
- [16] S. K. Acharya and R. Khatri, JCAP **02**, 010 (2020), arXiv:1912.10995.
- [17] S. K. Acharya and R. Khatri, JCAP **06**, 018 (2020), arXiv:2002.00898.
- [18] M. Boudaud and M. Cirelli, Phys. Rev. Lett. **122**, 041104 (2019), arXiv:1807.03075.
- [19] S. Clark, B. Dutta, Y. Gao, Y.-Z. Ma, and L. E. Strigari, Phys. Rev. D **98**, 043006 (2018), arXiv:1803.09390.
- [20] A. Bhoonah, J. Bramante, F. Elahi, and S. Schon, Phys. Rev. Lett. **121**, 131101 (2018), arXiv:1806.06857.
- [21] A. Bhoonah, J. Bramante, F. Elahi, and S. Schon, Phys. Rev. D **100**, 023001 (2019), arXiv:1812.10919.
- [22] G. R. Farrar, F. J. Lockman, N. M. McClure-Griffiths, and D. Wadekar, Phys. Rev. Lett. **124**, 029001 (2020), arXiv:1903.12191.
- [23] D. Wadekar and G. R. Farrar, (2019), arXiv:1903.12190.
- [24] P. Lu *et al.*, (2020), arXiv:2007.02213.
- [25] E. V. Ryan-Weber *et al.*, Mon. Not. Roy. Astron. Soc. **384**, 53 (2008), arXiv:0711.2979.
- [26] E. A. K. Adams and T. A. Oosterloo, A&A **612**, A26 (2018), arXiv:1712.06636.
- [27] E. N. Kirby *et al.*, ApJ **779**, 102 (2013), arXiv:1310.0814.
- [28] A. Sternberg, C. F. McKee, and M. G. Wolfire, Astrophys. J. Suppl. **143**, 419 (2002), arXiv:astro-ph/0207040.
- [29] Y. Faerman, A. Sternberg, and C. F. McKee, Astrophys. J. **777**, 119 (2013), arXiv:1309.0815.
- [30] F. Haardt and P. Madau, ApJ **746**, 125 (2012), arXiv:1105.2039.
- [31] B. T. Draine, *Physics of the interstellar and intergalactic medium*, Princeton series in astrophysics (Princeton University Press, Princeton, NJ, 2010).
- [32] L. Spitzer, *Physical processes in the interstellar medium* (, 1978).
- [33] A. G. G. M. Tielens, *The Physics and Chemistry of the Interstellar Medium* (, 2005).
- [34] S. Glover and T. Abel, Mon. Not. Roy. Astron. Soc. **388**, 1627 (2008), arXiv:0803.1768.
- [35] S. C. O. Glover, (2016), arXiv:1610.05679.
- [36] S. Bialy and A. Sternberg, ApJ **881**, 160 (2019), arXiv:1902.06764.
- [37] A. Dalgarno and R. McCray, Ann. Rev. Astron. Astrophys. **10**, 375 (1972).
- [38] J. H. Black, MNRAS **197**, 553 (1981).
- [39] M. Asplund, N. Grevesse, A. Sauval, and P. Scott, Ann. Rev. Astron. Astrophys. **47**, 481 (2009),



arXiv:0909.0948.

- [40] E. B. Jenkins, *ApJ***700**, 1299 (2009), arXiv:0905.3173.
- [41] M. L. Lykins *et al.*, *ApJ***807**, 118 (2015), arXiv:1506.01741.
- [42] S. S. Tayal, *A&A***486**, 629 (2008).
- [43] K. L. Bell, K. A. Berrington, and M. R. J. Thomas, *MNRAS***293**, L83 (1998).
- [44] P. S. Barklem, *A&A***462**, 781 (2007), arXiv:astro-ph/0609684.
- [45] K. M. Aggarwal and F. P. Keenan, *MNRAS***442**, 388 (2014), arXiv:1405.0184.
- [46] E. M. Verner *et al.*, *ApJS***120**, 101 (1999).
- [47] S. S. Tayal and O. Zatsarinny, *ApJS***188**, 32 (2010).
- [48] Ā. Barinovs, M. C. van Hemert, R. Krems, and A. Dalgarno, *ApJ***620**, 537 (2005).
- [49] F. Lique, J. Kłos, M. H. Alexander, S. D. Le Picard, and P. J. Dagdigan, *MNRAS***474**, 2313 (2018).
- [50] D. N. Page, *Phys. Rev.* **D13**, 198 (1976).
- [51] D. N. Page, *Phys. Rev.* **D16**, 2402 (1977).
- [52] J. MacGibbon and B. Webber, *Phys. Rev. D* **41**, 3052 (1990).
- [53] A. Arbey and J. Auffinger, *Eur. Phys. J. C* **79**, 693 (2019), arXiv:1905.04268.
- [54] M. Ricotti, N. Y. Gnedin, and J. Shull, *Astrophys. J.* **575**, 33 (2002), arXiv:astro-ph/0110431.
- [55] J. M. Shull and M. E. van Steenberg, *Astrophys. J.* **298**, 268 (1985).
- [56] S. R. Furlanetto and S. J. Stoever, *MNRAS***404**, 1869 (2010), arXiv:0910.4410.
- [57] E. Dwek, *ApJ***501**, 643 (1998), arXiv:astro-ph/9707024.
- [58] A. Rémy-Ruyer *et al.*, *A&A***563**, A31 (2014), arXiv:1312.3442.
- [59] D. B. Fisher *et al.*, *Nature***505**, 186 (2014).
- [60] T. Totani, T. Morokuma, T. Oda, M. Doi, and N. Yasuda, *PASJ***60**, 1327 (2008), arXiv:0804.0909.
- [61] D. Maoz, F. Mannucci, and T. D. Brandt, *MNRAS***426**, 3282 (2012), arXiv:1206.0465.
- [62] L. C. Vargas, M. Geha, E. N. Kirby, and J. D. Simon, *ApJ***767**, 134 (2013), arXiv:1302.6594.
- [63] D. Webster, J. Bland-Hawthorn, and R. Sutherland, *ApJ***799**, L21 (2015), arXiv:1501.02799.
- [64] M. Jeon, G. Besla, and V. Bromm, *ApJ***848**, 85 (2017), arXiv:1702.07355.
- [65] M. J. Irwin *et al.*, *ApJ***656**, L13 (2007), arXiv:astro-ph/0701154.
- [66] J. T. A. de Jong *et al.*, *ApJ***680**, 1112 (2008), arXiv:0801.4027.
- [67] D. R. Weisz *et al.*, *ApJ***748**, 88 (2012), arXiv:1201.4859.
- [68] J. D. Simon, *ARA&A***57**, 375 (2019), arXiv:1901.05465.
- [69] E. N. Kirby, G. A. Lanfranchi, J. D. Simon, J. G. Cohen, and P. Guhathakurta, *Astrophys. J.* **727**, 78 (2011), arXiv:1011.4937, [Erratum: *Astrophys. J.* 750, 173 (2012)].
- [70] E. B. Jenkins and T. M. Tripp, *Astrophys. J.* **734**, 65 (2011), arXiv:1104.2323.
- [71] S. C. Madden, F. Galliano, A. P. Jones, and M. Sauvage, *A&A***446**, 877 (2006), arXiv:astro-ph/0510086.
- [72] R. W. Schunk and P. B. Hays, *Planet. Space Sci.***19**, 113 (1971).
- [73] J. M. Shull, *ApJ***234**, 761 (1979).
- [74] V. Berestetskii, E. Lifshitz, and L. Pitaevskii, *QUANTUM ELECTRODYNAMICS*, Course of Theo-

retical Physics Vol. 4 (Pergamon Press, Oxford, 1982).

- [75] F. L. Schöier, F. F. S. van der Tak, E. F. van Dishoeck, and J. H. Black, *A&A***432**, 369 (2005), [arXiv:astro-ph/0411110](https://arxiv.org/abs/astro-ph/0411110).